

# Blunting of cracks of intermediate states of stress by scanning electron microscopy

P. S. THEOCARIS, V. KYTOPOULOS, C. STASSINAKIS

*Department of Engineering Science, Athens National Technical University, P.O. Box 77230, Athens Gr175-10, Greece*

A study of ductile blunting edge cracks in tensile specimens was undertaken in this paper by detecting the forms of different stages of blunting of the cracks under conditions of mode-I deformation as the loading progressed. All three main types of blunting were detected, with identical specimens and cracks, that is, the rounded off, the multicornered and the pointed type, depending on the particular accidental instabilities appearing in the vicinity of the crack tip as the blunting process is progressing. It was shown that an intermediate type of blunting was detected on the surfaces of the specimens by the scanning electron microscope (SEM) and this was explained by the fact that at the surfaces of specimens possessing a significant thickness to width aspect ratio the state of stress at the surface is strongly influenced by the plane stress conditions prevailing at the lateral faces of the specimens.

## 1. Introduction

It is well known that ductile fracture, starting from a pre-existing crack, may be preceded by the following four phases: Blunting of the crack followed by the initiation of crack growth, which then evolves into stable crack propagation and ends with unstable and rapid crack propagation.

The qualitative and the quantitative evolution of the previously mentioned phases are dependent on the properties of the materials and the geometry of the specimens, as well as on the geometry of the crack.

Whatever macroscopic parameter is used to characterize these four phases, its relation to the crack growth increment  $\Delta a$  will be of the form shown in Fig. 1. One can see that the four phases of ductile fracture are reflected in four distinct regions of the curve. Some of these are macroscopic manifestations of microscopic changes in the material close to the tip.

The first two phases play an important role in fracture mechanics, because they define some fracture parameters. In linear elastic fracture mechanics (LEFM), Irwin's stress intensity factor,  $K$ , provides the necessary fracture parameter, the critical value of which in plane-strain opening mode is the fracture toughness  $K_{IC}$ . The  $K_{IC}$  approach is, however, applicable in the small scale yielding region only (SSY). So, outside this region of LEFM some other parameters must be introduced, as the J-integral [1] and the crack opening displacement (COD) [2], which attempt to interpret the plastic fracture of the materials.

Since the critical value of the COD has been proposed as a constant for materials by Wells [2], a lot of experimental, fractographical and mechanical methods have been developed and improved, but later it was proved that the direct and accurate measurement of the COD is very difficult if not impossible [3]. However, in the first stages of fracture procedure,

where the velocity of the propagating crack is not very high, the method of reflected caustics [4] yields excellent results for the COD of the lateral faces of the specimen measured exactly on the moving tip of the crack.

Moreover, the accurate measurement and the nature of the evolution of COD is directly related to the qualitative and quantitative evolution of the blunting. In particular, the existing theories for blunting, such as the theory of Rice-Johnson [5], Pelloux [6], and McMeeking [7], are related to the concept of a blunting line which is constructed indirectly and quite inconsistently [8].

Another interesting quantity for fracture mechanics, which is also difficult to measure, is the crack increment or stretching,  $\Delta a$ , during the first phase of crack growth [9].

While Rice and Johnson studied the case of blunting for plane strain cracked plates, Saka, Abé and Tanaka [11] solved, numerically, cases of mixed mode deformation of edge cracked plates under plane strain conditions. By studying the slip line fields around cracks of different inclinations they showed that blunting under mixed modes of deformation yields cracks whose flanks form shapes of "Japanese sword" type.

Blunting under plane stress conditions is much more complicated than under plane-strain conditions, since in this case the slip-line field created around the blunted crack affords only six relationships for its solution, while the number of unknowns are seven. In order to address this difficulty Theocaris's method [12] was based on the form of the deformed cracks in plane stress and the slip line field created around the crack tip, which was detected experimentally by using scanning electron microscopy and z-modulation of the microscope. In this way, and for the first time, slip-line

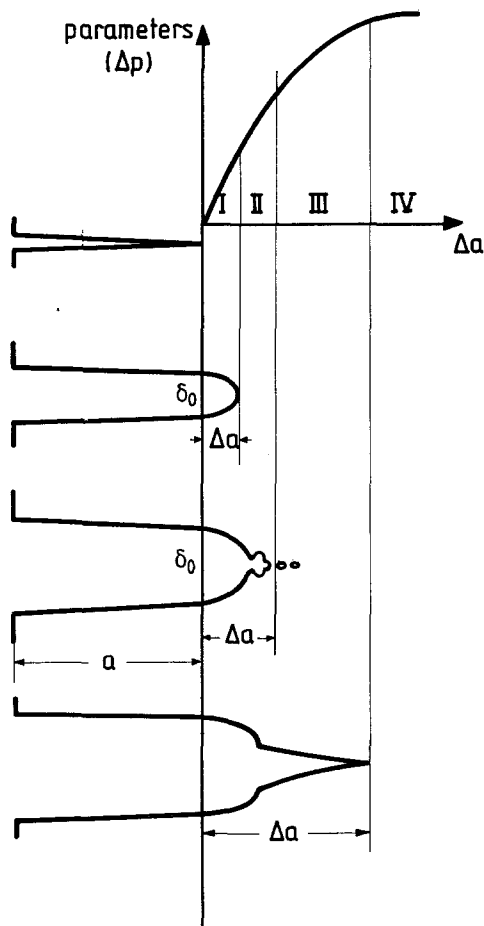


Figure 1 Load stretching diagram indicating the four characteristic phases of crack evolution (I) blunting, (II) initial crack growth, (III) stable crack propagation and (IV) unstable crack propagation.

fields of cracks under mixed mode and plane stress conditions were presented and interesting differences between the cases of plane strain and plane stress were established.

Taking into consideration the above remarks, we introduce in the present paper an experimental method of direct measurement of COD and  $\Delta a$  in the case of ductile fracture by means of measurements with the scanning electron microscope (SEM). The fundamental rationale and the advantages of the present method can be summarized as follows:

- i) The SEM can practically focus "intimately near" the crack tip, thus permitting an observation of extremely fine details,
- ii) Small size specimens may be used, not asking for special preparations, and
- iii) Observations can be made under off-, or on-load conditions.

In this paper, using the SEM, measurements were executed during the early stages of crack propagation, which were related especially to CODs and  $\Delta a$ s. From these measurements the blunting line was constructed for the materials tested and it was compared with existing blunting theories. As test material the polycarbonate (PC) was chosen, since it presents a significant amount of plasticity before fracture and shows blunting processes and forms with clear and sharp boundaries along the crack lips.

## 2. Theoretical background

In the small-scale yielding model introduced by Wells [2] and the Dugdale strip yielding based models [10], there is an implicit assumption that the COD occurs at both the original crack tip and the elastic-plastic boundary. However, nothing is implied regarding radial displacements ahead of the crack tip.

By considering shear strains in relation to the Prandtl field, Rice and Johnson [5] predicted for plane strain conditions that the crack tip would be deformed by radial displacements, such that for both small scale and large scale yielding the displacement tangentials to the original crack tip would be approximately doubling the respective displacement ahead of the position of the tip.

Pelloux [6] has proposed a simple model for the formation of the stretch zone at the crack tip. Moreover he found that shear initiates along a plane at  $45^\circ$  to the crack tip, until work-hardening makes further shear on another  $45^\circ$  plane more favourable. Thus deformation takes place by incremental shear that alternates between the two planes at  $45^\circ$  to the crack direction, so leading to an extension of the crack equal to half the crack flank opening displacement.

Later on, McMeeking [7], by using the method of finite elements for large geometric changes found different shapes for the blunting developed. In general, we can write:

$$\Delta a_{bl} = \lambda \delta_0 \quad (1)$$

where  $\Delta a_{bl}$  is the incremental crack extension and  $\delta_0$  is the COD, while the coefficient  $\lambda$  takes the values between 0.55 and 0.65 for the Rice-Johnson model, and the value 0.37 for the McMeeking model. By combining the above three models we can find a mean coefficient  $\bar{\lambda}$  with value of the order 0.5. The values of  $\lambda$  and  $\bar{\lambda}$ , as well as the above-mentioned models, concerned plane strain conditions. But, in the experimental situations it is rare to have pure plane strain or plane stress conditions. So it is necessary to introduce another important coefficient, which relates the plane strain and plane stress situation, which is the plastic constraint factor (PCF) [12] and which is defined by:

$$PCF = \frac{\sigma_{max}}{\sigma_{ys}} \quad (2)$$

where  $\sigma_{max}$  is the maximum applied stress and  $\sigma_{ys}$  is the yield stress of the material, while the quantity  $(PCF)\sigma_{ys}$  is defined as the effective yield stress.

For non-hardening materials  $PCF = 1.0$  for plane stress and  $PCF = 3$  for plane strain. For strain-hardening materials the PCF is different for each material and increases with increasing hardening exponent of the material.

## 3. Experimental details

Specimens of polycarbonate (PC) with elastic modulus  $E = 2.7 \cdot 10^8 \text{ Nm}^{-2}$  and Poisson's ratio  $\nu = 0.34$  were used. Their dimensions were: thickness  $d = 0.003 \text{ m}$ , width  $w = 0.006 \text{ m}$  and free length  $L_0 = 0.030 \text{ m}$ . An initial crack was machined by means of a razor blade. The ratio between the crack length  $a$ , and the width,  $w$ , was varied, within these limits:  $0.1 <$

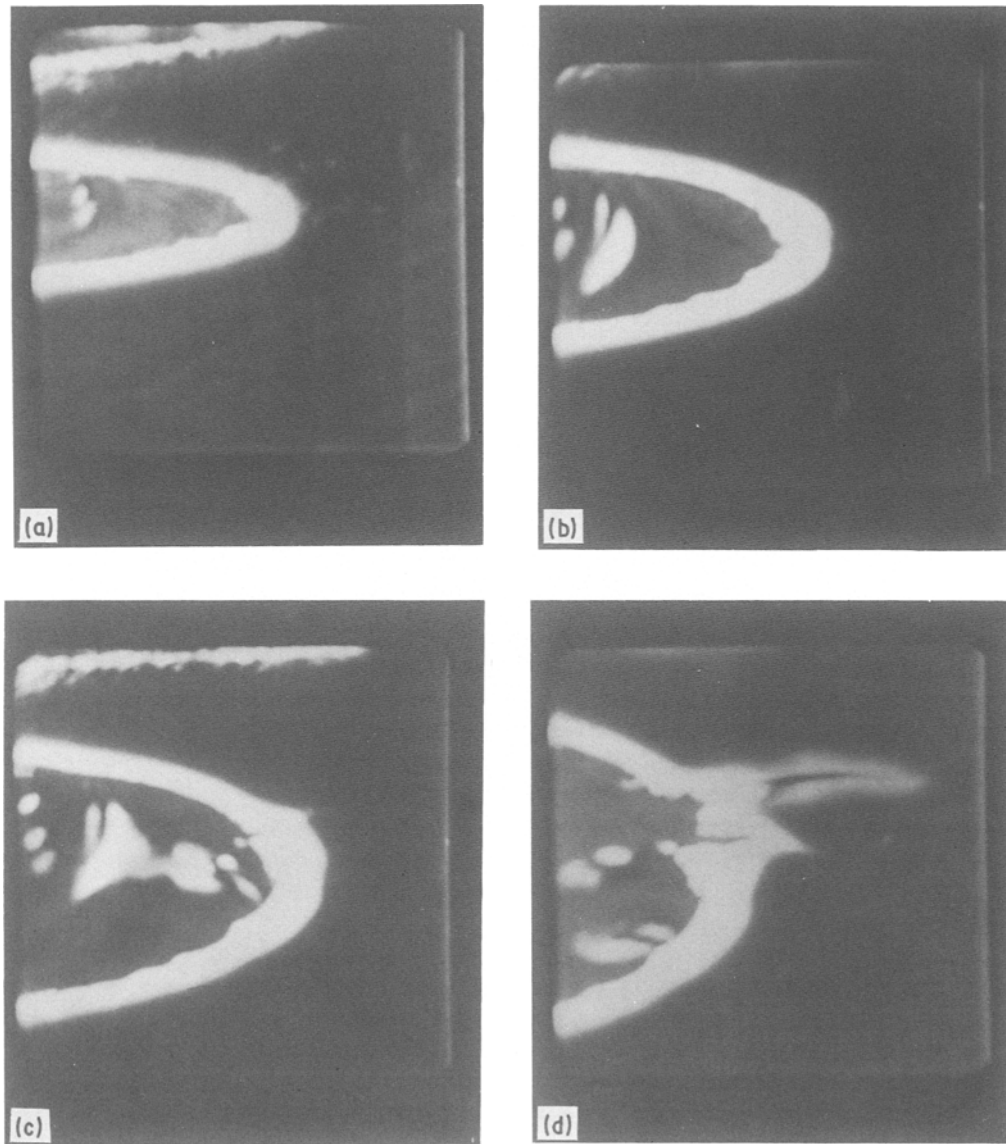


Figure 2 Electron scan micrographs indicating the evolution of phase I smooth blunting for three loading steps (a, b, c) and the beginning of phase II of the initiation of crack growth, (d). (a)  $\sigma_{\text{net}} \approx 15 \times 10^{-6} \text{ N m}^{-2}$ , (b)  $\sigma_{\text{net}} \approx 25 \times 10^{-6} \text{ N m}^{-2}$ , (c)  $\sigma_{\text{net}} \approx 33 \times 10^{-6} \text{ N m}^{-2}$ , (d)  $\sigma_{\text{net}} \approx 41 \times 10^{-6} \text{ N m}^{-2}$ . All micrographs are magnified by a factor of 1000;  $a \approx 2.7 \text{ mm}$ ,  $w \approx 7.0 \text{ mm}$ ,  $a/w = 0.4$ .

$a/w < 0.6$ . The specimens were covered with a thin film of aluminium coating to avoid charging phenomena from the electron beam. By means of a digital film thickness monitor (type FTM3, Edwards E306, London) the film thickness was kept constantly equal to 10 nm. It must be noted that the film of aluminium is not only protective, but also plays the role of a tracker, since it was cracked along slip-lines the densities of which depended on the intensities of strains developed in areas around the crack tips.

The observation of the specimens was performed with a scanning electron microscope of the type Cambridge S4-10 (Cambridge Ltd.) furnished with a special loading apparatus inside the chamber, for passing the bundle of electrons, called a tensile specimen stage. The observation and photographing was performed with jaw velocity  $0.2 \text{ mm min}^{-1}$  of the loading apparatus. The SEM parameters were: beam voltage 20 kV, beam current 200 mA, filament current 3.5 A and maximum load capacity 2350 N.

The specimens were put inside the tensile specimen stage of the microscope and submitted to a constant strain rate. At each loading step of the specimens the

crack tip zones were photographed, using a magnification factor of between 200 and 2000. From the study of these photographs the COD and the increase of the crack length were measured, and conclusions were derived concerning the blunting profile of the deformed cracks. Also from the photographs sufficient information for the study of the qualitative and quantitative evolution of the blunting phenomenon was obtained.

#### 4. Experimental results and discussion

In Figs 2, 3 and 4 a series of photographs were presented where the variation of the COD is detected for increasing load steps of the specimens. In all the three cases studied the ratio  $a/w$  was kept constant at a value of 0.4 and the dimensions of the specimens were identical. The magnification factor for Fig. 2 is 1000 and for Figs 3 and 4 is 500. Also, for the four consecutive steps in Fig. 2 the net section stress ( $\sigma_{\text{net}}$ ) had the values  $15 \times 10^{-6} \text{ N m}^{-2}$ ,  $25 \times 10^{-6} \text{ N m}^{-2}$ ,  $33 \times 10^{-6} \text{ N m}^{-2}$  and  $41 \times 10^{-6} \text{ N m}^{-2}$  respectively. The respective values of  $\sigma_{\text{net}}$  for the remaining Figs 3 and 4 were  $4 \times 10^{-6} \text{ N m}^{-2}$ ,  $20 \times 10^{-6} \text{ N m}^{-2}$ ,

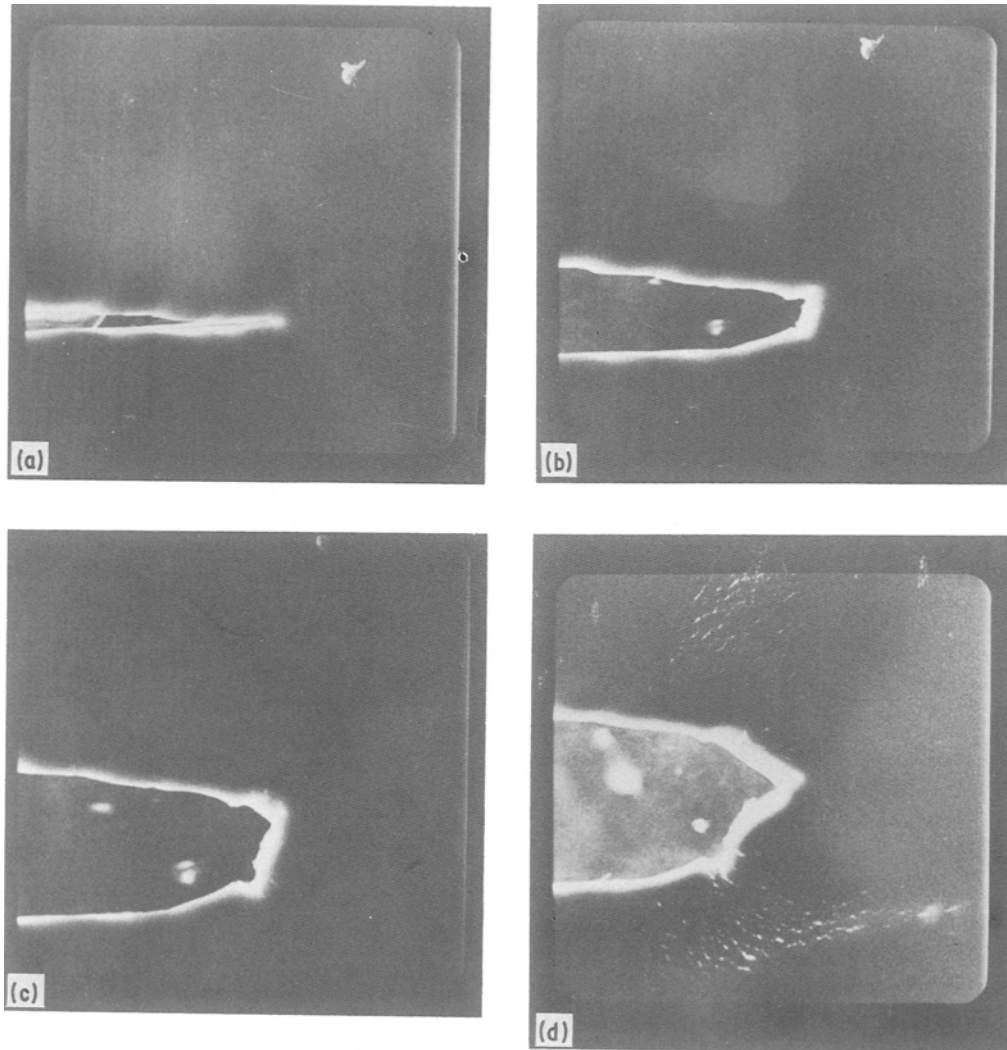


Figure 3 Electron scan micrographs indicating the evolution of phase I blunting with corners for three loading steps (a, b, c) and the beginning of phase II of the initiation of crack growth, (d). (a)  $\sigma_{\text{net}} \approx 4.0 \times 10^{-6} \text{ N m}^{-2}$ , (b)  $\sigma_{\text{net}} \approx 20 \times 10^{-6} \text{ N m}^{-2}$ , (c)  $\sigma_{\text{net}} \approx 30 \times 10^{-6} \text{ N m}^{-2}$ , (d)  $\sigma_{\text{net}} \approx 37 \times 10^{-6} \text{ N m}^{-2}$ . All micrographs are magnified by a factor of 500;  $a \approx 2.6 \text{ mm}$ ,  $w \approx 7.0 \text{ mm}$ ,  $a/w = 0.4$ .

$30 \times 10^{-6} \text{ N m}^{-2}$  and  $37 \times 10^{-6} \text{ N m}^{-2}$  for Fig. 3 and  $15 \times 10^{-6} \text{ N m}^{-2}$ ,  $22 \times 10^{-6} \text{ N m}^{-2}$  and  $30 \times 10^{-6} \text{ N m}^{-2}$  for Fig. 4. From the above cases the change in the crack shape is clearly seen and corresponds to the blunting phenomenon observed before crack propagation.

Although the dimensions of the specimens, the ratio  $a/w$  and the load conditions are kept identical in all the above three cases, one can distinguish three different blunting shapes. In Fig. 2, blunting is quite round, in Fig. 3 it shows many corners, whilst that of Fig. 4 has the so-called pointed shape. The observed blunting shapes agree well with those reported by McClintock [14], who has observed the opening of a macroscopic notch by a mechanism of shearing at two corners while Clayton and Knott [15] have observed localized shearing at many corners on a macroscopic notch tip. On the other hand, Rawal and Gurland [16] have observed the smooth mechanism of blunting at the opening of a pre-fatigued crack in spheroidized steel.

It is worthwhile noting that from the whole series of experiments we have executed, 55% developed smooth blunting, 32% blunting with corners and the remaining 13% pointed shape blunting. A possible explanation is that during the initial steps of crack

formation various local irregularities are created driving to different blunting types. This explanation agrees with the conclusion in [17] that the type of blunting which arises in a specific case may depend on strain-hardening and the tendency of deformation to localize at asperities close to the tip surface. Also in agreement is the difference in the blunting mechanism due to the difference in stress and strain distribution around the crack tip, in turn due to conditions of plane strain or plane stress.

In Fig. 5 (a and b) the blunted shape of a slant crack is also shown, where the upper crack tip has stronger curvature compared to that of the lower crack tip, which tends to remain sharp. This phenomenon, described previously by Saka, Abé and Tanaka [11] as the Japanese sword shape for plane strain cases, and discussed extensively by Theocaris [12] for plane stress oblique cracks seems to be universal, appearing in all ductile cracks under the influence of mode I and mixed mode deformations.

Figs 6 and 7 present the quantitative development of blunting  $\Delta a$ , plotted against the COD,  $\delta_0$ , and  $\sigma_{\text{net}}$  respectively for experiments with smooth blunting only.

From Fig. 7 it may be concluded that the variation of  $a/w$  does not affect the relationship between  $\Delta a_{\text{bl}}$

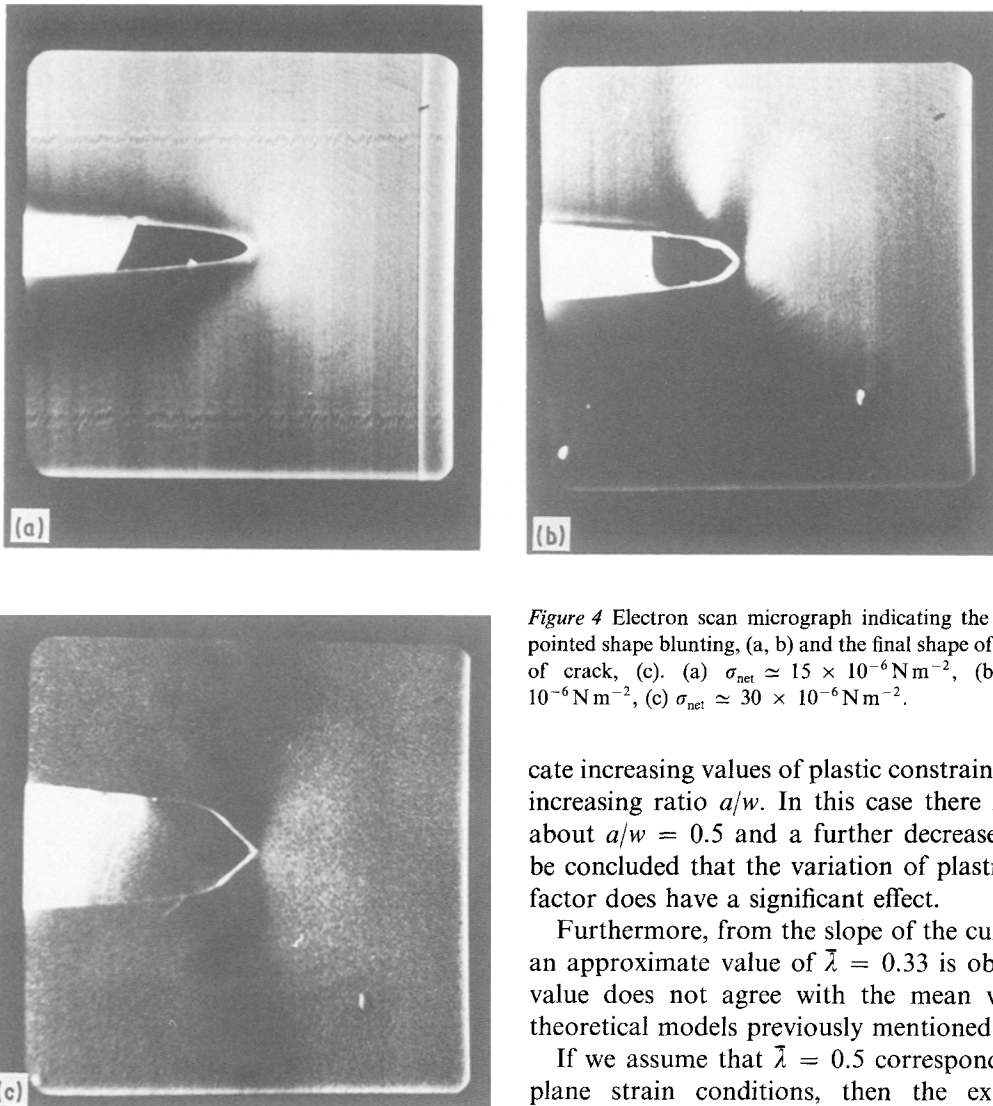


Figure 4 Electron scan micrograph indicating the evolution of a pointed shape blunting, (a, b) and the final shape of a V-type shape of crack, (c). (a)  $\sigma_{\text{net}} \approx 15 \times 10^{-6} \text{ N m}^{-2}$ , (b)  $\sigma_{\text{net}} \approx 22 \times 10^{-6} \text{ N m}^{-2}$ , (c)  $\sigma_{\text{net}} \approx 30 \times 10^{-6} \text{ N m}^{-2}$ .

cate increasing values of plastic constraint factor with increasing ratio  $a/w$ . In this case there is a peak at about  $a/w = 0.5$  and a further decrease. So it may be concluded that the variation of plastic constraint factor does have a significant effect.

Furthermore, from the slope of the curve of Fig. 7 an approximate value of  $\bar{\lambda} = 0.33$  is obtained. This value does not agree with the mean value of the theoretical models previously mentioned.

If we assume that  $\bar{\lambda} = 0.5$  corresponds to perfect plane strain conditions, then the experimentally measured value of  $\bar{\lambda} = 0.33$  corresponds to a mixed state of only 66% of perfect plane strain and the rest is plane stress. Thus, our experiments represent a mixed plane stress and plane strain state. These observations agree with experimental data with small scale yielding [20] and the empirical statements of Irwin [21] concerning the evaluation of the plastic zone, as well as recent experimental evidences stated in [11] and [12].

and  $\delta_0$ . It could be expected, taking into consideration the work of Milne and Chell [18], where the in-plane constraint described by  $k_j$  is sensitive to  $a/w$ , and therefore that blunting would also be sensitive to  $a/w$ . But, as it was theoretically shown by Ewing-Richards [19], the predictions of slip-line field theories for SENT (single-edge notched tensile) geometries indi-

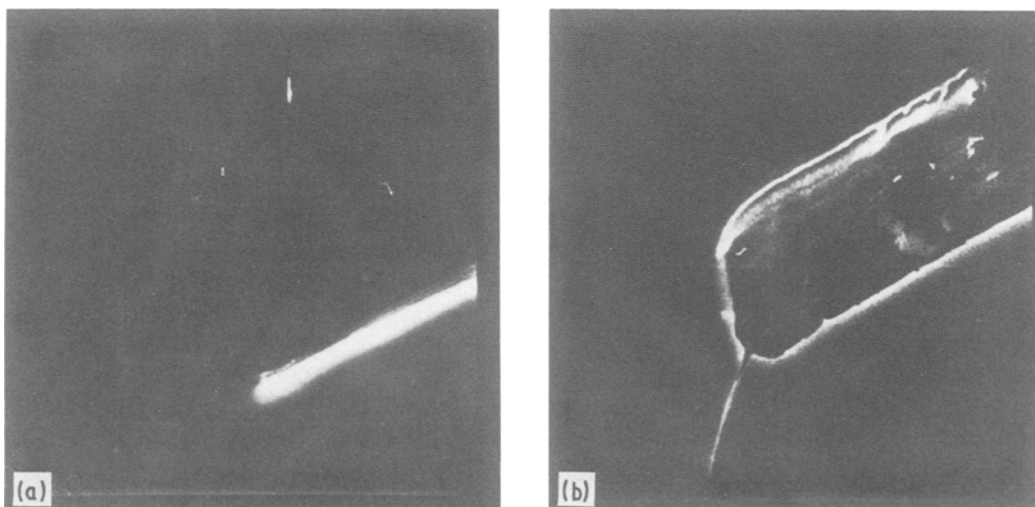


Figure 5 Electron scan micrographs for blunting of the Japanese sword type for an initially slanting crack.

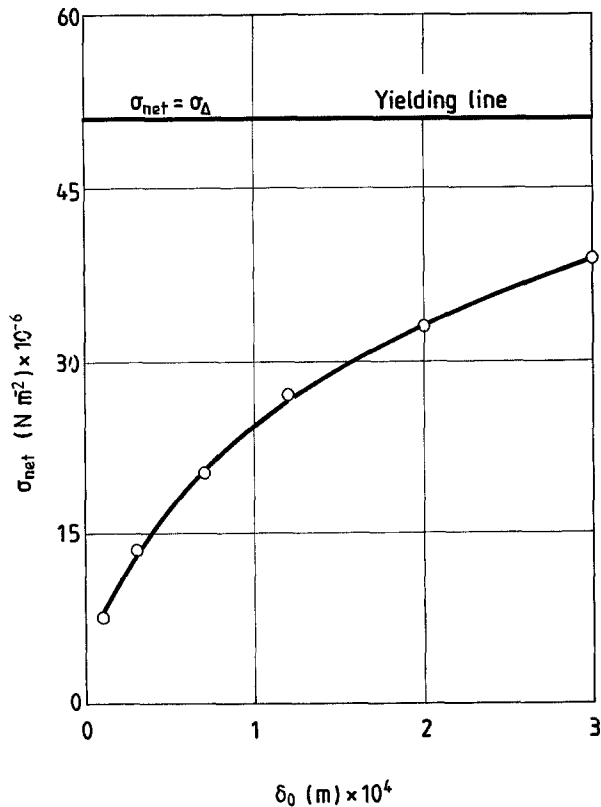


Figure 6 Evolution of the COD,  $\delta_0$ , due to blunting versus the average stress,  $\sigma_{net}$ ,  $a/w = 0.43$ .

The above results are connected with the kind of measurements obtained by SEM. Really, only surface variations are observed and measured by SEM, only surface variations are observed and measured, where the external layers of the material are close to plane stress conditions and the effective yield stress is lower than that in the middle plane of the specimen width, where plane strain holds. The difference in the yield stress value between surface and middle layers of the material causes different modes of blunting evolution. In this way the difference between the present experimental results and those of [22–24] is explainable. The latter results were obtained by using the Robinson–Tetelman, heat tinting and stereographical methods respectively, i.e. they are concentrated at the middle planes of the specimens, where plane strain dominates, whereas the present data correspond to the specimen surface where plane stress conditions are prevalent.

The values of  $\sigma_{net}$  and  $\delta_0$  of Fig. 6 form a straight line in a  $\log \sigma_{net}$  against  $\log \delta_0$  plot with slope equal to  $1/2$ , which implies that  $\delta_0 \sim \sigma_{net}^2$ . It is known that this relationship between  $\delta_0$  and  $\sigma_{net}$  is expressed by the Dugdale model, which is valid for  $\sigma_{net} < \sigma_{ys}$ , a restriction not violated in Fig. 6, where the whole curve lies below the yielding line.

Finally, it must be noted that our experiments do not point to a simple and uniform type of blunting through the thickness of the specimen, but only to a surface concentrated blunting, since all our measurements were restricted to the surface of the specimens.

## 5. Conclusions

The experimental study described above points to the following conclusions:

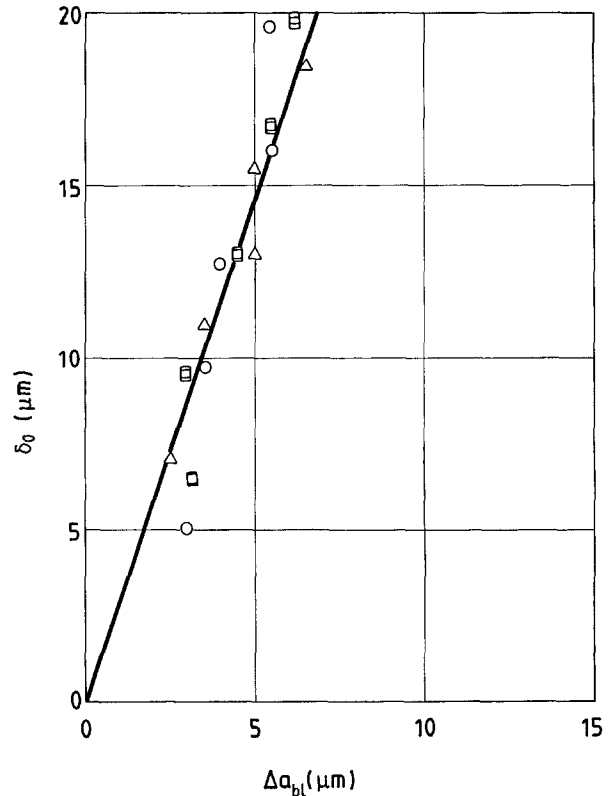


Figure 7 Variation of the COD,  $\delta_0$ , versus the stretching  $\Delta a_{bl}$  for parametric values of  $a/w$ . ( $\square$ )  $a/w = 0.1$ , ( $\circ$ )  $a/w = 0.2$ , ( $\triangle$ )  $a/w = 0.6$ .

(i) During the blunting phase, any one of the three blunting shapes, either round, with corners, or pointed, may be formed under identical specimen geometries and load conditions. This is because at the initial stages of crack forming many irregularities are created around the crack tip leading to different forms of blunting. Furthermore, since the thickness of the specimens in general is comparable to their width and the initial crack length, pure plane stress or plane strain conditions are difficult, if not impossible to establish.

(ii) The ratio  $a/w$ , namely the in-plane constraint, does not affect the relationship between  $\Delta a_{bl}$  and  $\delta_0$ .

(iii) The experimental relationship between COD and  $\sigma_{net}$  verifies the Dugdale equation, when  $\sigma_{net} < \sigma_{ys}$ .

(iv) The coefficient,  $\lambda$ , relating  $\Delta a_{bl}$  and  $\delta_0$ , takes experimental values not coinciding with its value according to the theoretical models. This is due to the fact that theoretical models assume plane strain states, whilst experimental measurements were performed on the surface of the specimens, where surface blunting prevails and plane stress conditions interfere which conceal the pure plane strain conditions valid at middle surfaces of thick specimens.

## References

1. J. A. BEGLEY and J. D. LANDES, "Fracture Toughness", Part III, ASTM STP 514 (American Society for Testing and Materials, Philadelphia, 1972).
2. A. A. WELLS, "Crack Propagation Symposium", College of Aeronautics, Cranfield, 1, (1961) p. 210.
3. C. G. CHIPPERFIELD, *Int. J. Fract.*, **12** (1976) 873.
4. P. S. THEOCARIS, *J. Strain Analysis* **9** (1974) 197.
5. J. R. RICE and M. A. JOHNSON, *Inelastic Behaviour of Solids* (1970) 641.

6. R. M. N. PELLOUX, *Engng Fract. Mech.* **1** (1970) 697.
7. R. M. McMEEKING, *J. Mech. Phys. Solids* **25** (1977) 357.
8. W. D. CAO and X. P. LU, *Int. Jnl. Fract.* **25** (1984) 33.
9. D. BROEK, *Engng Fract. Mech.* **6** (1974) 173.
10. G. T. HAHN and A. R. ROSENFELD, *Acta Metall.* **13** (1965) 293.
11. M. SAKA, H. ABE and S. TANAKA, *Comp. Mechanics* **1** (1986) 11.
12. P. S. THEOCARIS, *Engng Fract. Mech.* **32** (4) (1988) 354.
13. D. BROEK, "Elementary Engng Fracture Mechanics" (Noordhoff Inter. Publishing, Leyden, 1974) p. 105.
14. F. A. McCLINTOCK, "Fracture" edited by H. Liebowitz (Academic, New York) **3** (1970) 47.
15. J. Q. CLAYTON and J. F. KNOTT, *Met. Sci.* **10** (1976) 63.
16. S. P. RAWAL and J. GURLAND, in Proceedings of the 42nd International Conference on Mechanical Behaviour of Materials, Boston, 16–20 August 1976, pp. 1154.
17. F. A. McCLINTOCK, "Fracture", edited by H. Liebowitz (Academic, New York) **3** (1970) 158.
18. J. MILNE and G. G. CHELL, ASTM STP 668 (American Society for Testing and Materials, Philadelphia, 1979) p.358.
19. D. J. F. EWING and C. E. RICHARDS, *J. Mech. Phys. Sol.* **22** (1974) 27.
20. G. T. HAHN and A. R. ROSENFELD, *ASTM Trans.* **59** (1966) 909.
21. G. R. IRWIN, in Proceedings of the 7th Sagamore Conference (John Wiley, New York, 1960) 63.
22. B. A. FIELDS and K. J. MILLER, *Engng Fract. Mech.* **9** (1977) 137.
23. WU-SHAH-XIAN, *Engng Fract. Mech.* **18** (1) (1983) 83.
24. C. M. GILMORE, *Met. Sci.* **17** (1983) 177.

*Received 5 February  
and accepted 13 June 1988*